

Enhancement of Anion Recognition Exhibited by a Zinc-Imidazole-Based Ion-Pair Receptor Composed of C-H Hydrogen- and Halogen-Bond donor Groups

Received 00th January 20xx,

Paula Sabater,^a Fabiola Zapata,^a Bernardo López,^a Israel Fernández,^b Antonio Caballero *^a and Pedro Molina *^a

Accepted 00th January 20xx

DOI: 10.1039/x0xx00000x

www.rsc.org/

A 2-haloimidazole-tetraphenylethylene ion-pair receptor **1** is shown to recognise only HSO₄⁻ anions in the presence of a cobound Zn²⁺ cation guest species, which induced a remarkable increase with concomitant blue shift of the emission band of the complex [1·2Zn]⁴⁺ whereas no affinity of the free receptor **1** by the anions is observed. In addition, the downfield shifts observed by ¹H NMR of the H_a, H_b and H_c protons of the complex [1·2Zn]⁴⁺ upon the addition of HSO₄⁻ anions indicate their participation in the recognition event. According to DFT studies upon chelating a Zn²⁺ cation with two imidazole nitrogen atoms, the receptor **1** adopts a conformation ideally fitted to recognise HSO₄⁻ through a combination of C(sp₂)-H...O and C(sp₃)-H...O hydrogen bondings, C(sp₂)-Br...O halogen bonding and C(sp₂)...O tetrel bonding.

Introduction

The synergetic effects in the design and synthesis of ditopic receptors containing binding sites for both cationic and anionic species, that is, ion-pair recognition receptors, is an advancing area of research.¹ In recent years, combinations of cooperative noncovalent interactions have vastly increased the number of highly selective and sensitive receptors able to detect anions in aqueous and biological media.² Among various noncovalent interactions, hydrogen bonding is arguably the most important one and has been studied extensively from both theoretical and experimental points of view. In recent years, a similar type of noncovalent interaction, halogen bonding, has attracted much attention. It refers to a highly directional supramolecular noncovalent interaction between a Lewis-acidic region of a halogen atom X and a highly electro-negative atom Y in the form of R-X...Y-R.³ Applications of convergent hydrogen and halogen bond donor groups for anion recognition in the field of the ion-pair recognition is, however, very limited.⁴

Due to its amphoteric nature, the imidazole ring can function as a selective and effective anion and/or cation receptor.⁵ In fact, the imidazole ring behaves as an excellent hydrogen bond donor moiety in synthetic anion receptor systems. On the other hand, the presence of a donor pyridine-like nitrogen atom within the ring,

capable of selectively binding cationic species also converts the imidazole derivatives into excellent metal cation sensors. In addition, the acidity of the C(2)-H protons of the imidazole ring increases upon coordination to the metal centre, due to the electron withdrawing effect of the metal cation. In this context, the 2-haloimidazolium unit has been widely employed as a potent binding site for a variety of anions.⁶

Recently, it has been reported that the tetraphenylethylene core (TPE) is one of the most accessible and simplest AIE-type chromophores (aggregation-induced emission), which is of crucial importance to make more efficient and more sensitive fluorescence turn-on sensors from rotor-containing chromophores.⁷ Herein, we describe the synthesis and a comparative study of ion-pair sensing properties of two different ion-pair receptors, **1** and **2** (Figure. 1) bearing 2-Br-imidazoles or imidazoles, respectively, as the only binding site.

To this end, we have combined in a highly preorganized system the fluorogenic behaviour of the central tetraphenylethylene core and the binding ability of the imidazole ring. These receptors demonstrate a dramatic enhancement of anion binding by a cobound cation, whereas no affinity for anions is observed in the free receptors. The basic nitrogen atoms of the imidazole rings act

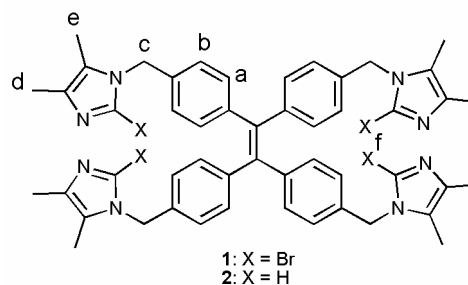


Figure 1. Structure of the ion-pair receptors **1** and **2**.

^a Departamento de Química Orgánica, Universidad de Murcia, Campus de Espinardo, 30100, Murcia, Spain.

^b Departamento de Química Orgánica I and Centro de Innovación en Química Avanzada (ORFEO-CINQA), Facultad de Ciencias Químicas, Universidad Complutense, E-28040 Madrid, Spain.

Electronic Supplementary Information (ESI) available: NMR spectra, fluorescence and ¹H-NMR anion binding studies and computational results See DOI: 10.1039/x0xx00000x

as cation binding sites while anions are mainly bonded to the preformed receptor-metal complex through halogen- or hydrogen-bonding interactions.

Results and discussion

Synthesis

The syntheses of the target ion-pair receptors **1** and **2** were accomplished from the reaction between the 1,1,2,2-tetrakis(4-(bromomethyl)phenyl)ethene⁸ and 2-bromo-4,5-dimethyl-1H-imidazole⁹ or 4,5-dimethyl-1H-imidazole,¹⁰ respectively, in basic medium. As expected, the yields obtained were low, 20% and 6.9% for the receptors **1** and **2** respectively due to the formation of by-products.

Ion-Pair Binding Studies

The ion-pair complexing properties of the receptors **1** and **2** have been investigated by emission techniques and ¹H NMR spectroscopy. Firstly, we evaluated the cation sensing properties of receptors **1** and **2** ($c = 1 \times 10^{-5} \text{ M}^{-1}$ in CH_3CN) by fluorescence spectroscopy toward various metal cations (Li^+ , Na^+ , K^+ , Ca^{2+} , Mg^{2+} , Cs^{2+} , Ni^{2+} , Cu^{2+} , Zn^{2+} , Cd^{2+} , Pb^{2+} , Fe^{3+} , Al^{3+} , Ag^+). The emission spectra of receptors **1** and **2** when excited at $\lambda = 330 \text{ nm}$ showed a low intensity emission band at $\lambda = 497 \text{ nm}$ and $\lambda = 482 \text{ nm}$, respectively, with a quantum yield of $\Phi = 3.4 \times 10^{-3}$ for receptor **1** and $\Phi = 1.7 \times 10^{-3}$ for receptor **2**. Only the stepwise addition of Zn^{2+} or Cd^{2+} cations to a solution of the receptors **1** or **2** induced a remarkable perturbation in their fluorescence spectra. The presence of Zn^{2+} or Cd^{2+} promotes an increase of the intensity of the emission band in the receptor **1** of 18-fold for Zn^{2+} cations and 12-fold for Cd^{2+} cations (Figure 2a). In addition, the quantum yields were also increased 17-fold and 11-fold for Zn^{2+} and Cd^{2+} , respectively.

The Job's plot experiments clearly indicate a 2:1 cation/receptor binding model. DynaFit analysis¹¹ of the titration data (see Supporting Information S12-S15) revealed that the receptor **1** binds Zn^{2+} ($K_1 = 4.3 \times 10^7 \text{ M}^{-1}$ and $K_2 = 5.3 \times 10^6 \text{ M}^{-1}$) more strongly than Cd^{2+} cations ($K_1 = 8.2 \times 10^4 \text{ M}^{-1}$ and $K_2 = 6.5 \times 10^4 \text{ M}^{-1}$). Interestingly, when the same experiments were performed on the imidazole receptor **2**, the results revealed a markedly different behaviour than that observed for the 2-Br-imidazole receptor **1**. Thus, whereas in 2-Br-imidazole receptor **1**, a continuous increase of the intensity of the emission band was observed until reaching the plateau (Figure 2b) a different behavior was observed for receptor **2** upon addition of two equivalents of the cations. In this case, the intensity of the emission band at $\lambda = 482 \text{ nm}$ increases during the addition up to 0.5 equivalents of Zn^{2+} or Cd^{2+} cations and subsequent addition of these cations from 0.5 to 2 equiv promotes a decrease of the intensity of the emission band (see Supporting Information S16-S17). This fact suggests the existence of different complexes with different stoichiometries and emission properties of the receptor **2** with Zn^{2+} and Cd^{2+} cations.

The ability of the receptors **1** and **2** to sense anions was also evaluated by fluorescence spectroscopy. Thus, addition of the following anions $\text{HP}_2\text{O}_7^{3-}$, H_2PO_4^- , SO_4^{2-} , HSO_4^- , NO_3^- , F^- , Cl^- , Br^- , I^- ,

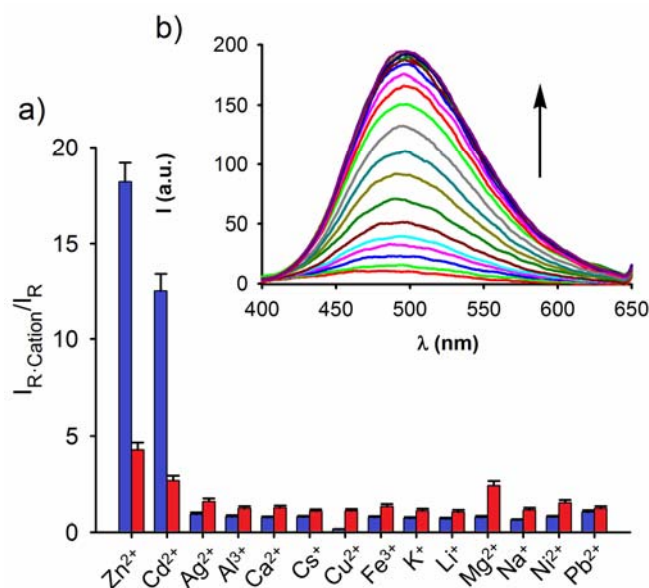


Figure 2. Graphical representation of the relative intensity of the emission band of receptors **1** (blue) and **2** (red) upon addition of 2 equiv of various cations in CH_3CN solution. Inset: Changes in the fluorescence spectrum of receptor **1** ($c = 1 \times 10^{-5} \text{ M}$ in CH_3CN) upon addition of Zn^{2+} cations. $\lambda_{\text{exc}} = 330 \text{ nm}$

AcO^- , ClO_4^- , BF_4^- , $\text{C}_6\text{H}_5\text{CO}_2^-$ and PF_6^- as tetrabutylammonium (TBA) salts to a solution of the receptors **1** or **2** ($c = 1 \times 10^{-5} \text{ M}$ in CH_3CN) did not cause any significant perturbation in their emission spectra therefore indicating that receptors **1** and **2** are not able to sense anions by themselves.

To evaluate the ion-pair sensing properties of the receptors **1** and **2** by fluorescence, Zn^{2+} cation was chosen as the cationic partner, since it was demonstrated that Zn^{2+} displayed the highest selectivity and affinity for these receptors (see above). The addition of the previously mentioned set of anions to a solution containing the preformed $[\mathbf{1}\cdot\mathbf{2Zn}]^{4+}$ complex ($c = 1 \times 10^{-5} \text{ M}$ in CH_3CN) causes three different effects (Figure 3a).

The most interesting response was observed after the addition of the HSO_4^- anion, which induced a remarkable increase (Figure 3, blue bar) with concomitant blue shift ($\Delta\lambda = -35 \text{ nm}$) of the emission band of the complex $[\mathbf{1}\cdot\mathbf{2Zn}]^{4+}$ at $\lambda = 497 \text{ nm}$ (Figure 3b). The maximum intensity and blue shift of the emission band were reached after the addition of 2 equiv and then remain unaltered upon the addition of a large excess of HSO_4^- anion. This behaviour could be attributed to a complexation process. The Job's plot experiments clearly indicate a 2:1 anion/receptor stoichiometry and the calculated association constants were found to be $K_1 = 2.2 \times 10^5 \text{ M}^{-1}$ and $K_2 = 3.4 \times 10^4 \text{ M}^{-1}$.

On the other hand, the presence of excess of $\text{HP}_2\text{O}_7^{3-}$, H_2PO_4^- , SO_4^{2-} , F^- , Cl^- , Br^- , AcO^- , and $\text{C}_6\text{H}_5\text{CO}_2^-$ causes an important decrease of the emission band of the complex $[\mathbf{1}\cdot\mathbf{2Zn}]^{4+}$ at $\lambda = 497 \text{ nm}$, which resembles the fluorescence of the uncomplexed receptor **1** (Figure 3, green bars). This fact could indicate that those anions sequester the Zn^{2+} cation from the receptor **1** forming the respective salt of zinc. Finally, NO_3^- , I^- , ClO_4^- , BF_4^- , and PF_6^- anions did not cause any kind of perturbation in the emission spectrum of $[\mathbf{1}\cdot\mathbf{Zn}]^{4+}$ (Figure 3 purple bars).

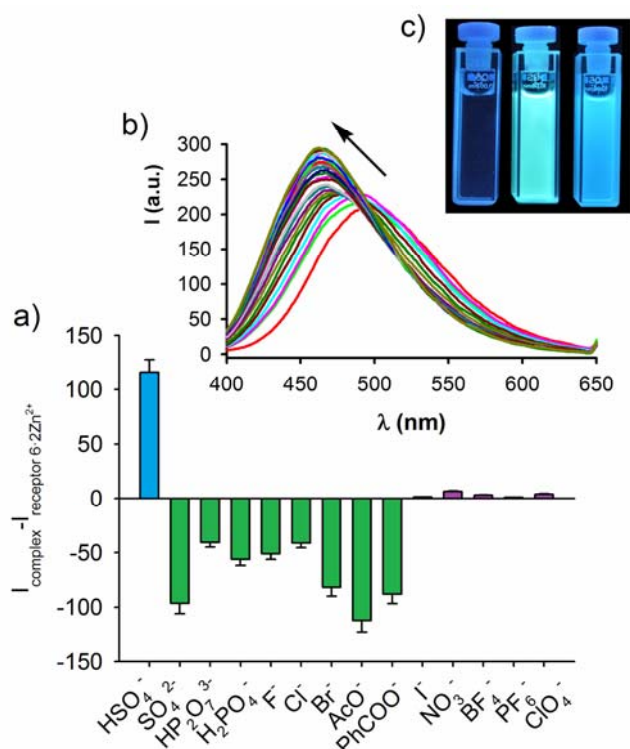


Figure 3. a) Modification of the intensity of the emission band of the complex [1·2Zn]⁴⁺ at $\lambda = 462$ nm upon addition of several anions. b) Changes in the fluorescence spectrum of the complex [1·2Zn]⁴⁺ ($c = 1 \times 10^{-5}$ M in CH₃CN) upon addition of HSO₄⁻ anion. c) Visual changes observed in the receptor **1** (left) upon the addition of Zn²⁺ (centre) and Zn(HSO₄)₂ (right). $\lambda_{\text{exc}} = 330$ nm

In contrast to the high selectivity showed by the halogenated complex [1·2Zn]⁴⁺ toward HSO₄⁻, fluorescence experiments carried out with the hydrogen-substituted counterpart [2·2Zn]⁴⁺ indicate that this complex does recognize HSO₄⁻, SO₄²⁻, and H₂PO₄⁻ with high association constant values, while the addition of excess of AcO⁻, PhCOO⁻ and F⁻ anions induced the disruption of the complex [2·2Zn]⁴⁺. HP₂O₇³⁻ anion represents a particular case, as the presence of this anion up to 2 equiv. produces an increase in the emission intensity, which can be attributed to an initial recognition process. However, the addition of an excess, more than two equivalents of the HP₂O₇³⁻ anion, cause the disruption of the complex indicated by the decrease of the fluorescence (see Supporting Information S30). The remaining NO₃⁻, I⁻, ClO₄⁻, BF₄⁻, and PF₆⁻ anions did not cause any perturbation in the emission spectrum of the [2·Zn]⁴⁺, as it was observed in the complex [1·2Zn]⁴⁺ (see Supporting Information S26-S33).

To further confirm that receptors **1** and **2** can be used for ion-pair recognition of Zn(HSO₄)₂, ZnSO₄ and Zn(H₂PO₄)₂, the simultaneous complexation of Zn²⁺ cation and the respective anion

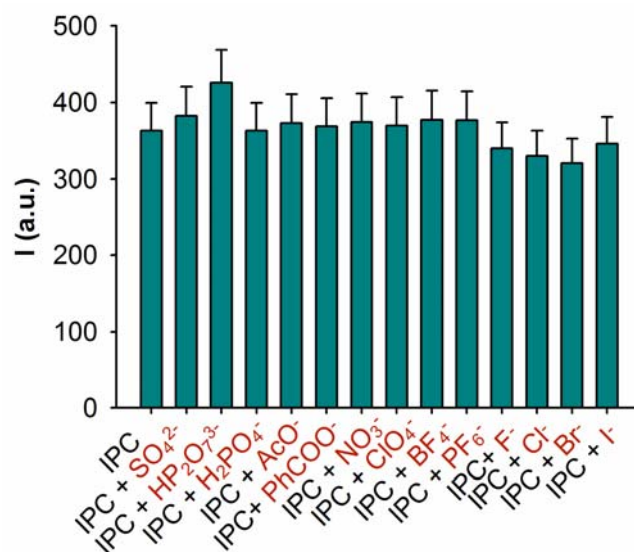


Figure 4. Competition experiments of the Ion Pair Complex [1·2Zn]⁴⁺+HSO₄⁻ (IPC) $c = 1 \times 10^{-5}$ M in CH₃CN with the addition of 1 equiv of several anions, monitoring the emission band at $\lambda = 462$ nm. $\lambda_{\text{exc}} = 330$ nm

was also investigated by fluorescence. The emission band obtained after the addition of Zn(HSO₄)₂ was identical to that observed by the sequential addition of Zn²⁺ cation and HSO₄⁻ anion confirming the ability of receptor **1** to sense Zn(HSO₄)₂. In the same way, the ability of receptor **2** to sense Zn(HSO₄)₂, ZnSO₄ and Zn(H₂PO₄)₂ was also demonstrated (see Supporting Information S-34-S37). Importantly, the formation of the ion-pairs could be monitored by naked-eye (Figure 3c).

Competition experiments were performed to test the specificity of the anion recognition by [1·2Zn]⁴⁺, ($c = 1 \times 10^{-5}$ M in CH₃CN) for HSO₄⁻ anions. The intensity of the emission band at $\lambda = 462$ nm of the ion pair [1·2Zn]⁴⁺+HSO₄⁻ remained practically unaltered with the addition of 1 equiv of SO₄²⁻, H₂PO₄⁻, AcO⁻, PhCOO⁻, NO₃⁻, ClO₄⁻, BF₄⁻, PF₆⁻ and I⁻ while the presence of 1 equiv of HP₂O₇³⁻, F⁻, Cl⁻, and Br⁻ anions promotes a weak increase of 17, 4, 6 and 9% respectively, in the intensity of the emission band at $\lambda = 462$ nm band (Figure 4).

In order to get detailed information about the ability of receptors **1** and **2** to form ion-pair complexes, ¹H NMR experiments were also performed in the solvent mixture CD₃CN/CD₃OD (9:1 v/v).

Receptors **1** and **2** have similar ¹H NMR spectra in CD₃CN/CD₃OD 9:1 the only exception is the presence of the imidazole proton H_f at $\delta = 7.43$ ppm in the hydrogen bond donor receptor **2** which is absent in the bromimidazole **1**. The methyl protons of the imidazole rings appear around $\delta \sim 2.00$ ppm, while the four methylene protons appear as a singlet around $\delta \sim 5.00$. and the phenyl H_a and H_b protons as a doublets in the aromatic region.

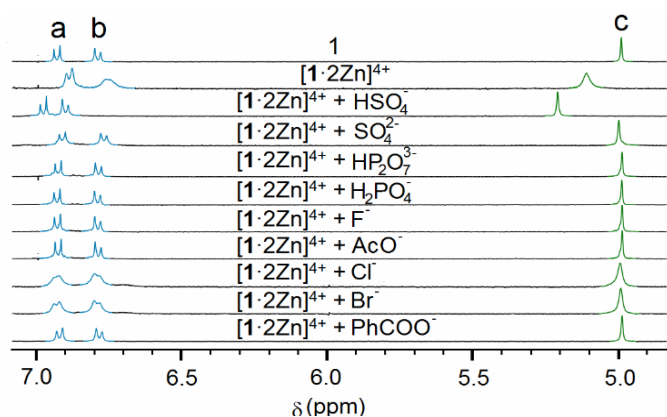


Figure 5. Changes observed in the ^1H NMR spectrum of **1** in $\text{CD}_3\text{CN}/\text{CD}_3\text{OD}$ (9:1 v/v) in the presence of the indicated species.

A comparative study of the ^1H NMR spectra between the free receptors **1** and **2** with the complexes formed upon the addition of 2 equiv of Zn^{2+} cation, i.e. $[\mathbf{1}\cdot 2\text{Zn}]^{4+}$ and $[\mathbf{2}\cdot 2\text{Zn}]^{4+}$, and after the addition of excess of several anions, confirms that complex $[\mathbf{1}\cdot 2\text{Zn}]^{4+}$ selectively recognizes HSO_4^- anion, as was evidenced by the downfield shift observed in the protons H_a ($\Delta\delta = 0.11$ ppm), H_b ($\Delta\delta = 0.17$ ppm) and H_c ($\Delta\delta = 0.13$ ppm). The accurate determination of the chemical shift of the protons H_d and H_e was not possible due to those signals become very broad in the presence of Zn^{2+} cations. Nevertheless, two clear singlet downfield shifted ($\Delta\delta_d = 0.23$, $\Delta\delta_e = 0.16$ ppm) respect to the receptor **1** were observed upon the addition of the HSO_4^- anions therefore indicating their participation in the recognition event (see Supporting Information S44). On the other hand, the presence of $\text{HP}_2\text{O}_7^{3-}$, H_2PO_4^- , SO_4^{2-} , F^- , Cl^- , Br^- , AcO^- and $\text{C}_6\text{H}_5\text{CO}_2^-$ regenerates the ^1H NMR spectrum of receptor **1** (Figure 5) without Zn^{2+} cation. This fact suggests the formation of the respective Zn salt instead of the ion-pair complex. On the other hand, complex $[\mathbf{2}\cdot 2\text{Zn}]^{4+}$ recognizes HSO_4^- , SO_4^{2-} and H_2PO_4^- as inferred by the observed downfield shifts in the H_f ($\Delta\delta \sim 0.9$ ppm), H_a ($\Delta\delta \sim 0.10$ ppm), H_b ($\Delta\delta \sim 0.2$ ppm) and H_c ($\Delta\delta \sim 0.2$ ppm) protons. In contrast, the following anions: $\text{HP}_2\text{O}_7^{3-}$, F^- , AcO^- and $\text{C}_6\text{H}_5\text{CO}_2^-$ cause the disruption of the complex (see Supporting Information S45). In both cases, NO_3^- , I^- , ClO_4^- , BF_4^- , and PF_6^- did no modify the ^1H NMR spectra of the complexes $[\mathbf{1}\cdot 2\text{Zn}]^{4+}$ and $[\mathbf{2}\cdot 2\text{Zn}]^{4+}$.

The low organosolubility of the metal complexes as well as the ion-pair complexes did not allow obtaining their respective ^{13}C NMR spectra.

Computacional Study

Density Functional Theory (DFT) calculations¹³ were carried out to gain more insight into both the structure of the complex formed between receptor $[\mathbf{1}\cdot 2\text{Zn}]^{4+}$ and HSO_4^- and the nature of the interactions established between these species. Due to the symmetry of receptor **1**, we used a model initial receptor **1'** having the 1,1,2,2-tetrakis(phenyl)ethene core and only two 2-bromoimidazole groups. The coordination of the nitrogen atoms of the imidazole rings to $\text{Zn}(\text{ClO}_4)_2$ leads to the formation of the $[\mathbf{1}'\cdot \text{Zn}(\text{ClO}_4)]^+$ complex (Figure 6). This species may adopt two different conformations which are nearly isoenergetic (see

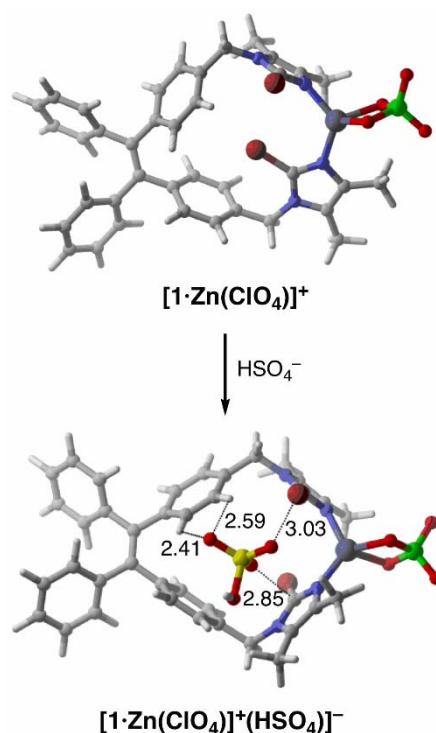


Figure 6. Fully optimized geometries of species $[\mathbf{1}'\cdot \text{Zn}(\text{ClO}_4)]^+$ and $[\mathbf{1}'\cdot \text{Zn}(\text{ClO}_4)]^+\cdot \text{HSO}_4^-$. Bond distances are given in angstroms. All data have been computed at the B3LYP-D3/def2-SVPP level.

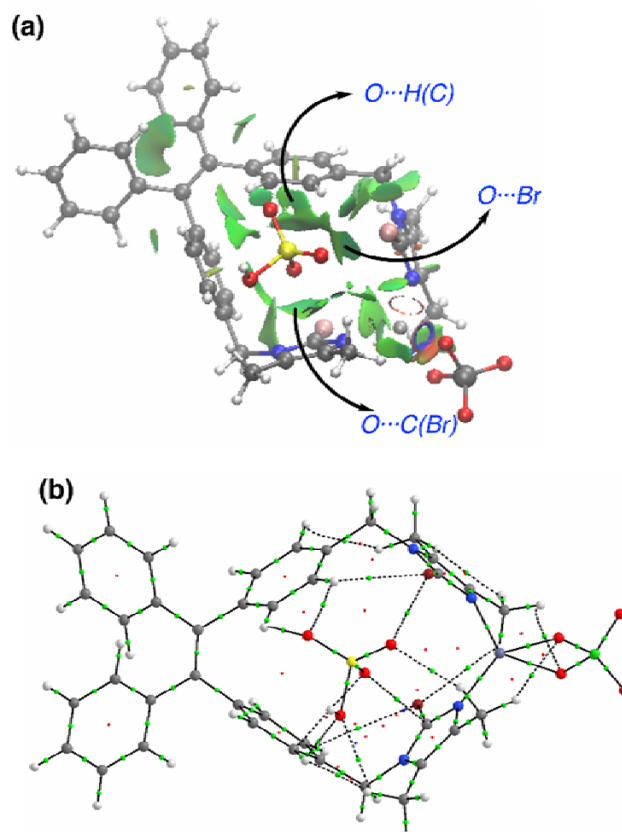


Figure 7. a) Representation of non-covalent interactions (a) and AIM diagram (b) computed for ion-pair $[\mathbf{1}'\cdot \text{Zn}(\text{ClO}_4)]^+\cdot \text{HSO}_4^-$. Green surfaces (top) indicate weak attractive non-covalent interactions. The lines connecting the nuclei (bottom) diagram are the bond paths, while the small green spheres indicate the corresponding bond critical points.

Supporting Information). The addition of the HSO_4^- anion to this species leads to the formation of the ion-pair complex $[\mathbf{1}'\text{-Zn}(\text{ClO}_4)]^+\text{-HSO}_4^-$. Not surprisingly, the optimized geometry of this ion-pair clearly indicates that receptor $[\mathbf{1}'\text{-Zn}(\text{ClO}_4)]^+$ modifies its initial equilibrium structure in order to accommodate the HSO_4^- anion. This is mainly possible by the presence of the methylene groups which allows the rotation of the imidazole groups. Complex $[\mathbf{1}'\text{-Zn}(\text{ClO}_4)]^+\text{-HSO}_4^-$ exhibits four main contacts (i.e. having distances shorter than the corresponding sum of van der Waals radii) between the anion and $[\mathbf{1}'\text{-Zn}(\text{ClO}_4)]^+$, namely $\text{C}(\text{sp}_2)\text{-Br}\cdots\text{O}$ (3.03 Å), $\text{C}(\text{sp}_2)\text{-H}\cdots\text{O}$ (2.41 and 2.59 Å), $\text{C}(\text{sp}_3)\text{-H}\cdots\text{O}$ (2.40 and 2.35 Å) and $\text{C}(\text{sp}_2)\cdots\text{O}$ (2.85 Å, see Figure 6). These $\text{O}\cdots\text{H}$ interactions are consistent with the shift observed for the protons H_a , H_b , H_d and H_e in the ^1H NMR experiments (see above). Interestingly, only one of the bromine atoms of the receptor is able to interact with the HSO_4^- anion. As a consequence of this $\text{C}(\text{sp}_2)\text{-Br}\cdots\text{O}$ interaction, the corresponding $\text{C}(\text{sp}_2)\text{-Br}$ bond becomes significantly shorter in the ion-pair complex with respect to the initial receptor (from 1.867 Å to 1.859 Å), whereas the non-interacting $\text{C}(\text{sp}_2)\text{-Br}$ remains mainly unaltered (1.868 Å).

The NCIPLOT method was then used to confirm and visualize the above mentioned non-covalent intermolecular interactions. As depicted in Figure 7a, these interactions are represented by green surfaces, which indicate the occurrence of non-covalent stabilizing interactions, namely $\text{C}(\text{sp}_2)\text{-H}\cdots\text{O}$ and $\text{C}(\text{sp}_3)\text{-H}\cdots\text{O}$ hydrogen bonding, $\text{C}(\text{sp}_2)\text{-Br}\cdots\text{O}$ halogen bonding and $\text{C}(\text{sp}_2)\cdots\text{O}$ tetrel bonding, between the anion and receptor. A similar scenario can be found by applying the Atom and Molecules (AIM) method. Indeed, the presence of these intermolecular interactions is also confirmed by the occurrence of bond-critical points associated with bond paths running between the atoms involved in these stabilizing interactions (Figure 7b). It can be then concluded that the combination of these weak (yet significant) intermolecular non-covalent interactions is, at least in part, responsible for the observed HSO_4^- recognition by the receptor $[\mathbf{1}\text{-Zn}]^{4+}$. In sharp contrast, the replacement of the bromine atoms by hydrogen atoms in receptor **2** leads to a completely different scenario, i.e. the anion is now mainly attached to the transition metal center (see Supporting Information S47), which is also consistent with the observed markedly different sensing properties of this receptor.

Conclusion

In conclusion, the 2-haloimidazole-tetraphenylethylene ion-pair receptor **1** exhibits a dramatic enhancement of HSO_4^- anion binding by cobound Zn^{2+} cations, whereas no affinity of the free receptor by anions is observed. Upon chelating a Zn^{2+} cation with two imidazole nitrogen atoms, the receptor adopts a conformation ideally fitted to recognise HSO_4^- through a combination of $\text{C}(\text{sp}_2)\text{-H}\cdots\text{O}$ and $\text{C}(\text{sp}_3)\text{-H}\cdots\text{O}$ hydrogen bonding, $\text{C}^+(\text{sp}_2)\text{-Br}\cdots\text{O}$ halogen bonding and $\text{C}(\text{sp}_2)\cdots\text{O}$ tetrel bonding. Receptor **1** shows a noticeable perturbation of its fluorescence properties in the presence of the HSO_4^- anion when the Zn^{2+} cation is attached to the imidazole binding site.

Experimental

The reactions were performed using dried solvents and the solvents were previously dried by the traditional method. All melting points were determined by means of a Kofler hot-plate melting-point apparatus and are uncorrected. Solution NMR spectra were recorded on NMR Bruker 200, 300, 400, or 600 MHz. The abbreviations used in the NMR data are the following s (singlet), m (multiplet), and q (quaternary carbon atom). Tetramethylsilane (TMS) has been used as internal reference to determinate the chemical shifts (δ) in the ^1H and ^{13}C NMR spectra. The concentration used in the UV-Vis and fluorescence titration stated in the text and in the corresponding figure captions, we have used a 10 mm path length cell with the spectra background corrected before and after sequential additions of different aliquots of anions. The stock solution of receptors **1** and **2** ($c = 1.0 \times 10^{-5}$ M) were prepared in CH_3CN and solution of different cations (Li^+ , Na^+ , K^+ , Ca^{2+} , Mg^{2+} , Cs^{2+} , Ni^{2+} , Cu^{2+} , Zn^{2+} , Cd^{2+} , Pb^{2+} , Fe^{3+} , Al^{3+} , Ag^+) and anions ($\text{HP}_2\text{O}_7^{3-}$, H_2PO_4^- , SO_4^{2-} , HSO_4^- , NO_3^- , F^- , Cl^- , Br^- , I^- , AcO^- , ClO_4^- , BF_4^- , $\text{C}_6\text{H}_5\text{CO}_2^-$ and PF_6^-) were also prepared in HPLC grade CH_3CN in 5 mL volumetric flask. The fluorescent studies were carried by the addition of aliquots of the cation or anions solution to the fluorescence cuvette containing a solution of the receptors **1** or **2**.

The value of the quantum yield were calculated using anthracene as the standard ($\Phi = 0.27 \pm 0.01$) and the following equation $\Phi_x/\Phi_s = (S_x/S_s) [(1 - 10^{-A_s})/(1 - 10^{-A_x})](n_s^2/n_x^2)$, where x and s indicate the unknown and standard solution, respectively, Φ is the quantum yield, S is the area under the emission curve, A is the absorbance at the excitation wavelength and n is the refractive index. ESI-MS spectra were recorded on a Agilent 6300 LC/MS Ion Trap VL.

Synthesis of 1,1,2,2-tetrakis(4-((2-bromo-4,5-dimethyl-1H-imidazol-1-yl)methyl)phenyl)ethane 1: Yield (62 mg, 20 %) To a solution of 2-bromo-4,5-dimethyl-1H-imidazole (0.23 g, 1.3 mmol) in acetonitrile (15 mL) was added dropwise a solution of 1M NaOH (1.3 mmol) and stirred during 10 min. 1,1,2,2-tetrakis(4-(bromomethyl)phenyl)ethane (0.2 g, 0.28 mmol) was added in one portion and the resultant mixture was stirred three days. The solvent was removed and the resultant residue dissolved in dichloromethane (100 mL), which was washed with water (2 x 25 mL). The aqueous layers were re-extracted with 25 mL dichloromethane, and the combined organic layers dried over magnesium sulphate, filtered and dried in vacuo. The mixture was purified by column chromatography (elution with 95:5 $\text{CH}_2\text{Cl}_2/\text{MeOH}$) to give the product as a yellow solid: ^1H NMR ($\text{CD}_3\text{CN}/\text{MeOD}$ 9:1, 400 MHz): δ_{H} 6.92 (8H, d, $J = 8$ Hz, H_a), 6.78 (8H, d, $J = 8$ Hz, H_b), 5.01 (8H, s, H_c), 2.07 (12H, s, H_d), 1.96 (12H, s, H_e) ppm; ^{13}C NMR ($\text{CD}_3\text{CN}/\text{MeOD}$ 9:1, 100 MHz): δ_{C} 143.7, 141.7, 135.7, 135.1, 132.4 (C_a), 127.6, 126.9 (C_b), 117.6, 49.32 (C_c), 12.46 (C_d), 9.56 (C_e) ppm; MS (ESI): m/z calc. for $[\text{M} + \text{H}]^+$ 1081.07, found 1081.07.

Synthesis of 1,1,2,2-tetrakis(4-((4,5-dimethyl-1H-imidazol-1-yl)methyl)phenyl)ethane 2: Yield (15 mg, 6.9 %) To a solution of 2-bromo-4,5-dimethyl-1H-imidazole (0.16 g, 1.6 mmol) in acetonitrile (15 mL) was added dropwise a solution of 1M NaOH (1.6 mmol) and stirred during 10 min. 1,1,2,2-tetrakis(4-(bromomethyl)phenyl)ethane (0.2 g, 0.28 mmol) was added in one portion and the resultant mixture was stirred three days. The solvent was removed and the resultant residue dissolved in

dichloromethane (100 mL), which was washed with water (2 x 25 mL). The aqueous layers were re-extracted with 25 mL dichloromethane, and the combined organic layers dried over magnesium sulphate, filtered and dried in vacuo. The mixture was purified by column chromatography (elution with 9:1 CH₂Cl₂/MeOH) to give the product as a white solid: ¹H NMR (CD₃CN/MeOD 9:1, 400 MHz), δ_H 7.43 (4H, s, H_f), 6.93 (8H, d, J = 8 Hz, H_a), 6.84 (8H, d, J = 8 Hz, H_b), 4.96 (8H, s, H_c), 2.06 (12H, s, H_d), 1.87 (12H, s, H_e) ppm; ¹³C NMR (CD₃CN/MeOD 9:1, 100 MHz): δ_C 150.04, 144.1, 136.9, 136.8 (C_f), 134.3, 132.6 (C_a), 127.8 (C_b), 124.2, 49.32 (C_c), 12.71 (C_d), 8.78 (C_e) ppm; MS (ESI): m/z calc. for [M + H]⁺ 765.43, found 765.43.

Computational Details. All the calculations reported in this paper were performed with the Gaussian 09 suite of programs.¹⁴ Electron correlation was partially taken into account using the hybrid functional usually denoted as B3LYP¹⁵ in conjunction with the D3 dispersion correction suggested by Grimme et al.¹⁶ using the double-ζ quality plus polarization def2-SVPP¹⁷ basis set for all atoms. All species were characterized by frequency calculations,¹⁸ and have positive definite Hessian matrices, thus confirming that they are minima on the potential energy surface.

Associated content

Supporting Information. ¹H and ¹³C NMR spectra, fluorescence anion binding studies, Job plot experiments, ¹H NMR experiments, computational details and Cartesian coordinates are available free of charge via the Internet at <http://pubs.acs.org>.

Author information

Corresponding Authors

antocaba@um.es

pmolina@um.es

Conflicts of interest

There are no conflicts to declare.

Acknowledgements

This work was funded by the Ministerio de Economía y Competitividad of Spain and FEDER (projects CTQ2013-46096-P, CTQ2017-86775-P, CTQ201235513-C0202, CTQ2016-78205-P and CTQ2016-81797-REDC). Fundación Séneca Región de Murcia (CARM) (projects 18948/JLI/13 and 19337/PI/14). P.S. acknowledges the University of Murcia for a FPU predoctoral grant.

Notes and references

- (a) S. K. Kim and J. L. Sessler, *Chem. Soc. Rev.*, 2010, **39**, 3784-3809; (b) A. J. McConnel and P. D. Beer, *Angew. Chem., Int. Ed.*, 2012, **51**, 5052-5061; (c) P. A. Gale, *Coord. Chem. Rev.*, 2003, **240**, 191-221.
- P. Molina, F. Zapata and A. Caballero, *Chem. Rev.*, 2017, **117**, 9907-9972.
- (a) G. Cavallo, P. Metrangolo, R. Milani, T. Pilati, A. Primagi, G. Resnati and G. Terraneo, *Chem. Rev.*, 2016, **116**, 2478-2601; (b) L. C. Gilday, S. W. Robinson, T. A. Barendt, M. J. Langton, B. R. Mullaney and P. D. Beer, *Chem. Rev.*, 2015, **115**, 7118-7195.
- (a) R. Tepper, B. Schulze, P. Bellstedt, J. Heidler, H. Görls, M. Jäger and U. S. Schubert, *Chem. Commun.*, 2017, **53**, 2260-2263; (b) A. Brown, K. M. Mennie, O. Mason, N. G. White and P. D. Beer, *Dalton Trans.*, 2017, **46**, 13376-13385.
- P. Molina, A. Tárraga and F. Otón, *Org. Biomol. Chem.*, 2012, **10**, 1711-1724.
- (a) A. Caballero, N. G. White and P. D. Beer, *Angew. Chem. Int. Ed.*, 2011, **50**, 1845-1848; (b) F. Zapata, A. Caballero, N. G. White, T. D. W. Claridge, P. J. Costa, V. Félix and P. D. Beer, *J. Am. Chem. Soc.*, 2012, **134**, 11533-11541 (c) P. Sabater, F. Zapata, A. Caballero, N. de la Visitación, I. Alkorta, J. Elguero and P. Molina, *J. Org. Chem.*, 2016, **81**, 7448-7458. (d) C. J. Serpell, N. L. Kilah, P. J. Costa, V. Felix and P. D. Beer, *Angew. Chem. Int. Ed.*, 2010, **49**, 5322-5326; (e) M. Cametti, K. Raatikainen, P. Metrangolo, T. Pilati, G. Terraneo and G. Resnati, *Org. Biomol. Chem.*, 2012, **10**, 1329-1333; (f) N. Schulz, P. Sokkar, E. Engele, S. Schindler, M. Erdelyi, E. Sanchez-Garcia and S. M. Huber, *Chem. Eur. J.*, 2018, **24**, 3464-3473.
- C. Y. K. Chan, Z. J. Zhao, J. W. Y. Lam, J. Z. Liu, S. M. Chen, P. Lu, F. Mahtab, X. J. Chen, H. H. Y. Sung, H. S. Kwok, Y. G. Ma, I. D. Williams, K. S. Wong and B. Z. Tang, *Adv. Funct. Mater.*, 2012, **22**, 378-389.
- Y. X. Zhu, Z. W. Wei, M. Pan, H. P. Wang, J. Y. Zhang and C. Y. Su, *Dalton Trans.*, 2016, **45**, 943-950.
- C. J. Serpell, N. L. Kilah, P. J. Costa, V. Félix and P. D. Beer, *Angew. Chem. Int. Ed.*, 2010, **49**, 5322-5326.
- A. D'Sa and L. A. Cohen, *J. Heterocycl. Chem.*, 1991, **28**, 1819-1820.
- P. Kuzmic, *Anal. Biochem.*, 1996, **237**, 260-273.
- During the titration a precipitate was present and therefore a quantitative analysis was not possible.
- All the calculations were carried out at the B3LYP-D3/def2-SVPP level. See ESI for further computational details.
- M. J. Frisch, G. W. Trucks, H. B. Schlegel, G. E. Scuseria, M. A. Robb, J. R. Cheeseman, G. Scalmani, V. Barone, B. Mennucci, G. A. Petersson, H. Nakatsuji, M. Caricato, X. Li, H. P. Hratchian, A. F. Izmaylov, J. Bloino, G. Zheng, J. L. Sonnenberg, M. Hada, M. Ehara, K. Toyota, R. Fukuda, J. Hasegawa, M. Ishida, T. Nakajima, Y. Honda, O. Kitao, H. Nakai, T. Vreven, J. A. Montgomery, Jr., J. E. Peralta, F. Ogliaro, M. Bearpark, J. J. Heyd, E. Brothers, K. N. Kudin, V. N. Staroverov, R. Kobayashi, J. Normand, K. Raghavachari, A. Rendell, J. C. Burant, S. S. Iyengar, J. Tomasi, M. Cossi, N. Rega, J. M. Millam, M. Klene, J. E. Knox, J. B. Cross, V. Bakken, C. Adamo, J. Jaramillo, R. Gomperts, R. E. Stratmann, O. Yazyev, A. J. Austin, R. Cammi, C. Pomelli, J. W. Ochterski, R. L. Martin, K. Morokuma, V. G. Zakrzewski, G. A. Voth, P. Salvador, J. J. Dannenberg, S. Dapprich, A. D. Daniels, Ö. Farkas, J. B. Foresman, J. V. Ortiz, J. Cioslowski, and D. J. Fox, *Gaussian 09 Revision D.01* Gaussian, Inc., Wallingford CT, 2009
- (a) A. D. Becke, *J. Chem. Phys.* 1993, **98**, 5648; (b) C. Lee, W. Yang, R. G. Parr, *Phys. Rev. B* 1998, **37**, 785; (c) S. H. Vosko, L. Wilk, M. Nusair, *Can. J. Phys.* 1980, **58**, 1200.
- S. Grimme, J. Antony, S. Ehrlich, H. Krieg, *J. Chem. Phys.* 2010, **132**, 154104.
- F. Weigend, R. Alhrichs, *Phys. Chem. Chem. Phys.* 2005, **7**, 3297.
- J. W. Mclver, A. K. Komornicki, *J. Am. Chem. Soc.* 1972, **94**, 2625.